Silicon plasmon resonances in the local-density approximation

R. Daling* and W. van Haeringen
Eindhoven University of Technology, Department of Physics, P.O. Box 513, 5600 MB Eindhoven, The Netherlands

B. Farid
Cavendish Laboratory, Madingley Road, Cambridge CB3 OHE, United Kingdom
(Received 27 September 1991; revised manuscript received 13 January 1992)

As a continuation of earlier work, we present the results of a local-density-approximation-based calculation of some dielectric properties of silicon. In particular, we have calculated the plasmon-resonance line shape for $\mathbf{k}\rightarrow\mathbf{0}$ and the plasmon dispersion curves including local-field effects and exchange-correlation corrections. The results are compared with both our earlier empirical-pseudopotential results and experimental data.

I. INTRODUCTION

In a previous paper[1] we have expounded on an efficient numerical method, based on analytical continuation, to calculate dielectric matrices of a semiconductor. We used this method to obtain the random-phase-approximation (RPA) dielectric matrices of Si as a function of wave vector $\mathbf{k}$ and frequency ω. Subsequently we calculated the plasmon dispersion curves, including local-field effects (LFE's) at all considered wave vectors. The Si band structure, which is a basic ingredient in such calculations, was obtained by using the empirical pseudopotential method (EPM).

The EPM-based plasmon energies turned out to be larger than the experimentally determined plasmon energies and also showed a stronger dispersion as a function of wave vector than the experimental values. Moreover, the small anisotropy in the experimental plasmon dispersion relations along the Δ [$\mathbf{k}=(0,t,t)$] and Λ [$\mathbf{k}=(t,t,t)$] axes of the first Brillouin zone (1BZ) was not correctly reproduced in our calculations. In fact, the experimental energy of a plasmon oscillation with a wave vector along the Δ axis is somewhat larger than the energy of a plasmon oscillation with a wave vector of the same magnitude along the Λ axis, whereas the calculated plasmon energies displayed the opposite behavior.

Since it is known that the so-called exchange-correlation corrections to the RPA flatten the plasmon dispersion[2-7] we have included these corrections in our calculations. The results of these calculations are presented in this paper. In contrast to Ref. 1, we have not used an EPM band structure but a local-density-approximation (LDA) band structure in which *ab initio* ion pseudopotentials are used to construct the crystal potential. The advantage of working with the LDA instead of the EPM is that it offers a natural, though approximative, way to include the exchange-correlation corrections in the dielectric matrix.

In the next section we summarize briefly how the exchange-correlation corrections to the dielectric matrix are handled in the framework of the LDA. After that we present the results of our calculations. These results comprise the plasmon dispersion along the Δ and Λ axes of the 1BZ and the plasmon-resonance line shape ($\mathrm{Im}[\epsilon^{-1}_{\mathbf{KK}}(\mathbf{k},\omega)]$ as a function of ω) for $\mathbf{k}\rightarrow\mathbf{0}$. Moreover, although not of direct importance for the plasmon dispersion, we have included a figure in which we show how the energy-loss function at $\mathbf{k}=(0.5,0.5,0.5)$ is composed of two plasmon resonances. We end with some conclusions.

II. DIELECTRIC PROPERTIES IN THE LDA

In the LDA the one-electron Hamiltonian has the form

$$H=T+V_{\mathrm{cr}}+V_H(\rho)+V_{\mathrm{xc}}(\rho) \tag{1}$$

in which T is the kinetic-energy operator and V_{cr} is the crystal potential. The Hartree potential $V_H(\rho)$ and the so-called exchange-correlation potential $V_{\mathrm{xc}}(\rho)$, which are both functionals of the electron density ρ, account for the electron-electron Coulomb interaction.

If a many-electron system is perturbed by an external potential $\Phi_{\mathrm{ext}}(\omega)$ with frequency ω, the response of the electrons to this potential induces a so-called screening potential $\Phi_{\mathrm{scr}}(\omega)$ in addition to $\Phi_{\mathrm{ext}}(\omega)$. The total internal potential $\Phi_{\mathrm{int}}(\omega)=\Phi_{\mathrm{ext}}(\omega)+\Phi_{\mathrm{scr}}(\omega)$, which is set up in the system, is the sum of the external potential and the screening potential and will be linearly related to the external potential if this potential is weak. This is expressed in the following equation:

$$\Phi_{\mathrm{int}}(\omega)=\epsilon^{-1}(\omega)\Phi_{\mathrm{ext}}(\omega)\ , \tag{2}$$

in which $\epsilon^{-1}(\omega)$ is the inverse dielectric matrix.

In the LDA, or in general in density-functional theory (DFT), the dielectric matrix is given by (see, e.g., Ref. 8)

$$\epsilon(\omega)=1-\left[V_C+\frac{\delta V_{\mathrm{xc}}}{\delta\rho}\right]P_0(\omega)\ . \tag{3}$$

In this expression $\delta V_{\mathrm{xc}}/\delta\rho$ is the functional derivative of the exchange-correlation potential with respect to the electron density evaluated around the ground-state density. Furthermore, $V_C(=\delta V_H/\delta\rho)$ is the naked $1/r$ electron-electron Coulomb interaction and $P_0(\omega)$ is the

RPA polarization matrix. The term $(\delta V_{xc}/\delta\rho)P_0(\omega)$ is the so-called exchange-correlation correction to the dielectric matrix. The response of the many-electron system to an external field is influenced by the Coulomb interaction between electrons and holes which are created during the polarization process. The above-mentioned exchange-correlation corrections account for these interactions. If the exchange-correlation corrections are disregarded, we obtain the more common RPA expression

$$\epsilon(\omega)=1-V_C P_0(\omega) . \tag{4}$$

It has to be remarked that DFT, and thus the LDA to it, can formally only be used to calculate ground-state properties. Therefore Eq. (3) is, strictly speaking, only usable to calculate the exchange-correlation corrections to the static dielectric matrix ($\omega=0$). A rigorous calculation of exchange-correlation corrections to the plasmon energies, which are determined by the dielectric properties at nonzero frequency, requires in principle the use of energy-dependent exchange-correlation corrections.[18,19] In spite of this, we use Eq. (3) to do a calculation of exchange-correlation corrections to the plasmon energies of an inhomogeneous system.

In a plane-wave basis Eq. (3) takes the form

$$\epsilon_{\mathbf{K}_1\mathbf{K}_2}(\mathbf{k},\omega)=\delta_{\mathbf{K}_1\mathbf{K}_2}-\frac{e^2}{\epsilon_0}\frac{1}{|\mathbf{k}+\mathbf{K}|^2}P_{\mathbf{K}_1\mathbf{K}_2}(\mathbf{k},\omega) - \sum_{\mathbf{Q}}\left[\frac{\delta V_{xc}}{\delta\rho}\right]_{\mathbf{K}_1\mathbf{Q}}(\mathbf{k})P_{\mathbf{Q}\mathbf{K}_2}(\mathbf{k},\omega) . \tag{5}$$

In this expression $\mathbf{K}_1$, $\mathbf{K}_2$, and $\mathbf{Q}$ are reciprocal-lattice vectors and $\mathbf{k}$ is a vector in the 1BZ. The RPA expression for the polarization matrix $P_{\mathbf{K}_1\mathbf{K}_2}(\mathbf{k},\omega)$ in terms of the electron band structure is given by

$$P_{\mathbf{K}_1\mathbf{K}_2}(\mathbf{k},\omega)=\frac{2}{E_v a^3}I^0_{\mathbf{K}_1\mathbf{K}_2}(\mathbf{k},\omega) , \tag{6}$$

in which $I^0_{\mathbf{K}_1\mathbf{K}_2}(\mathbf{k},\omega)$ is the integral:

$$I^0_{\mathbf{K}_1\mathbf{K}_2}(\mathbf{k},\omega)=\int_{1BZ}d^3q\left[\sum_{l_1\in c}\sum_{l_2\in v}-\sum_{l_1\in v}\sum_{l_2\in c}\right]\frac{1}{\omega-\varepsilon_{l_1}(\mathbf{q})+\varepsilon_{l_2}(\mathbf{q}-\mathbf{k})\pm i\eta} \times\sum_{\mathbf{Q}_2}d_{l_1\mathbf{q}}(\mathbf{Q}_2)d_{l_2\mathbf{q}-\mathbf{k}}(\mathbf{Q}_2-\mathbf{K}_2)\sum_{\mathbf{Q}_1}d_{l_2\mathbf{q}-\mathbf{k}}(\mathbf{Q}_1-\mathbf{K}_1)d_{l_1\mathbf{q}}(Q_1) . \tag{7}$$

In Eq. (6), $a=5.43$ Å is the Si lattice constant and E_v is a unit of energy defined as $E_v=(2\hbar^2\pi^2)/(ma^2)=0.375$ Ry in which m is the electron mass. The $d_{l\mathbf{k}}(\mathbf{K})$ and $\varepsilon_l(\mathbf{k})$ are a plane-wave coefficient and band energy, respectively. Wave vectors are in units of $(2\pi)/a$ and energies in units of E_v; $l\in c$ or v means that the summation is to be done, respectively, over the conduction and valence bands only. In the energy denominator $+i\eta$ applies if $l_1\in c$ and $l_2\in v$, and $-i\eta$ applies if $l_1\in v$ and $l_2\in c$, where η is positive and infinitesimally small. Because we have chosen the origin of our coordinate system in a bond center between two Si atoms, the plane-wave coefficients in Eq. (7) are real. How we calculate the integral in Eq. (7) is discussed at length in Ref. 1.

We have to remark that although the exchange-correlation corrections are included in a way which is consistent with the LDA one-electron Hamiltonian, they suffer from a principal shortcoming which is due to the local nature of the LDA. Because of this local nature, the momentum representation $(\delta V_{xc}/\delta\rho)_{\mathbf{K}_1\mathbf{Q}}(\mathbf{k})$ is in fact independent of $\mathbf{k}$. This is an artifact of the LDA, however, and it is known from calculations on the free-electron gas that the $\mathbf{k}$ dependence of the exchange-correlation corrections can be important.[4,5]

In our calculations, the results of which will be presented in the next section, we have used the exchange-correlation potential that has been obtained in Ref. 9 by a fully self-consistent LDA calculation of the Si total ground-state energy. The exchange part of this potential has the Kohn-Sham form[10] and the correlation potential is according the the Wigner form.[11] The *ab initio* ion pseudopotential of Ref. 12 was used to construct the crystal potential V_{cr}.

III. RESULTS

In this section we present the results of our LDA calculations and we make a comparison with the EPM results of Ref. 1. In the remaining part of this paper we will use the shorthand notation "(S,N) LDA-EPM calculation" to indicate a LDA-EPM calculation in which we used an $S\times S$ dielectric matrix to account for the LFE and in which we used N plane waves in Eqs. (5)–(7) to calculate a dielectric matrix element $\epsilon_{\mathbf{K}_1\mathbf{K}_2}(\mathbf{k},\omega)$. We recall that all EPM calculations are done using Eq. (4), that is, no exchange-correlation corrections are included.

In Fig. 1(a) we have plotted the plasmon dispersion relations of Si along the Δ and Λ axes of the 1BZ as obtained in the energy-loss experiments of Refs. 13 and 14. Note that according to the experiments there is a small anisotropy in the dispersion along these two directions. The plasmon energy at a given $|\mathbf{q}|$ along the Δ axis is somewhat larger than the plasmon energy at the same $|\mathbf{q}|$ value on the Λ axis.

Figure 1(b) contains the calculated plasmon dispersion. The plasmon energies in this figure are the positions of the maxima in the calculated loss functions $-\mathrm{Im}[\epsilon^{-1}_{\mathbf{K}\mathbf{K}}(\mathbf{k},\omega)]$ (in Ref. 1 we called this the experimental definition). For the dispersion along both the Δ and the Λ directions two sets of results are shown. The symbols correspond to a (15,59) EPM calculation (□, Λ axis; +, Δ axis) and the lines (full line, Λ axis; dotted line, Δ

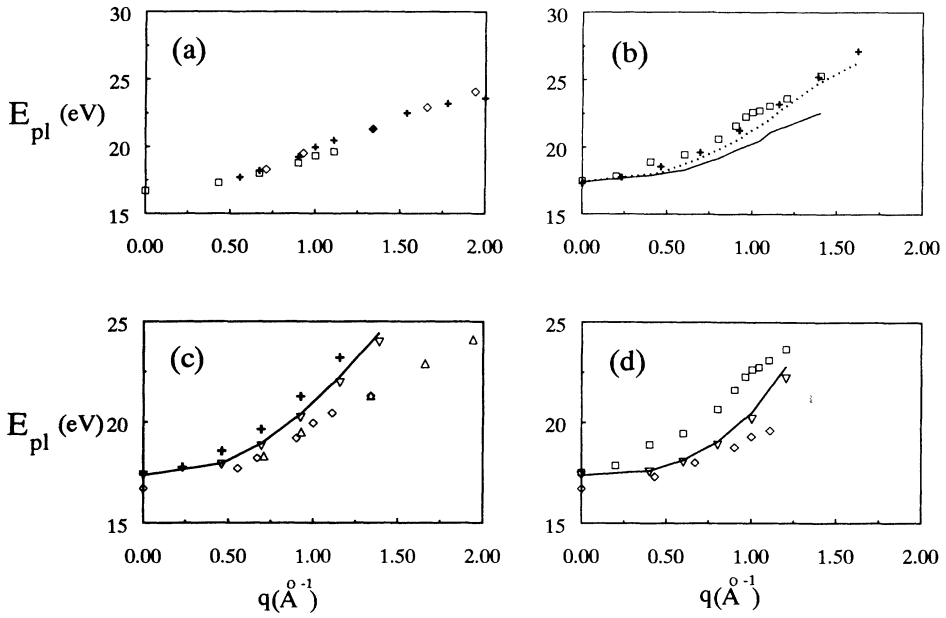

FIG. 1. Plasmon dispersion relations. (a) Experimental values. □, along Λ axis according to Ref. 13; ◇, along Δ axis according to Ref. 13; +, along Δ axis according to Ref. 14; (b) □, (15,59) EPM calculation along Λ axis; +, (15,59) EPM calculation along Δ axis; ——, (15,59) LDA calculation along Λ axis; · · · ·, (15,59) LDA calculation along Δ axis. (c) Plasmon dispersion along Δ axis. ◇, experiment according to Ref. 13; △, experiment according to Ref. 14; +, (15,59) EPM calculation of (b); ——, (27,113) LDA calculation; ∇, (27,113) LDA calculation with exchange-correlation corrections. (d) Plasmon dispersion along Λ axis. ◇, experiments according to Ref. 13; □, (15,59) EPM calculation of (b); ——, (27,113) LDA calculation; ∇, (27,113) LDA calculation with exchange-correlation corrections.

axis) have been obtained with a (15,59) LDA calculation according to Eq. (4), that is exchange-correlation corrections have not yet been included. Comparing in Fig. 1(b) the dotted line with the full line shows that the LDA plasmon energies along the Δ axis are somewhat larger than the LDA plasmon energies along the Λ axis. Thus we see that, in contrast to the EPM, the LDA leads to plasmon dispersion relations which display the experimentally observed anisotropy.

In Figs. 1(c) and 1(d) both the EPM- and LDA-based plasmon energies are compared with the experimental values. The full line in these figures corresponds to a (27,113) LDA calculation using Eq. (4). We observe that the LDA yields plasmon energies which are in far better agreement with experiment than the EPM plasmon energies. This is especially so for the plasmon energies along the Λ axis in Fig. 1(d). The ∇ symbols were obtained by taking exchange-correlation corrections into account according to Eq. (3). The effect of these corrections on the plasmon energies turns out to be very small and the plasmon dispersion is only slightly flattened in the direction of the experimentally determined dispersion.

The only small modification has to be contrasted with the much larger effect of exchange-correlation corrections on the plasmon dispersion which has been found in Refs. 4–7. Of these works Refs. 4–6 concern the free-electron gas and Ref. 7 (see Table I) deals with inhomogeneous systems. This larger effect of the exchange-correlation effects might be connected with the above-mentioned **k** independence of our exchange-correlation corrections, a shortcoming of which the cited works do not suffer. Moreover, as opposed to the LDA expression for the exchange-correlation correction $(\delta V_{xc}/\delta\rho)$ which we use, the exchange-correlation corrections in Refs. 4–7 are energy dependent and this energy dependence is important in the flattening of the plasmon dispersion.[6]

It is common usage to describe plasmon dispersion relations by

$$E_{pl}(\mathbf{q})=E_{pl}(\mathbf{0})+\alpha(\hbar^2/m)|\mathbf{q}|^2\ , \tag{8}$$

with α a dimensionless parameter. The RPA value of this parameter for the free-electron gas is given by $\alpha=\frac{3}{5}(E_F/\hbar\omega_0)$ with $\omega_0=E_{pl}(\mathbf{0})$ the plasmon frequency at $\mathbf{q}=\mathbf{0}$ and E_F the Fermi energy. If we use the free-electron gas expression for E_F in terms of the electron density ρ and substitute for ρ the value of the mean electron density in Si we find $\alpha=0.45$.

The results for a least-squares fit for α are given in Table I(a). In this table we make a distinction between the dispersion along the Δ axis (α_Δ) and the dispersion along the Λ axis (α_Λ). In the fit we have excluded the part of the dispersion relation at large $|\mathbf{q}|$, where the calculated plasmon energies start to deviate considerably from the experimental value. Accordingly, the plasmon energies at wave vectors up to $|\mathbf{q}|=0.93$ Å^{-1} were included in the fits for α_Δ and the plasmon energies at wave vectors up to $|\mathbf{q}|=0.8$ Å^{-1} were included in the fits for α_Λ.

Table I(a) shows that our LDA calculation reproduces

TABLE I. Values for the dimensionless dispersion coefficient α in Eq. (8). α_Δ and α_Λ are the coefficients for the dispersion along the Δ and Λ axes, respectively. The calculated plasmon energies up to $|\mathbf{q}|=0.93$ Å^{-1} were included in the fits for α_Δ and the plasmon energies up to $|\mathbf{q}|=0.80$ Å^{-1} in the fits for α_Λ. The value for α_Λ obtained by fitting to the EPM plasmon dispersion relation is marked with an * because this dispersion relation could not very well be described with Eq. (8). In (b) values obtained by other authors as well as the experimental values are given. (a) Calculated values from Ref. 15; (b1) calculated RPA values from Ref. 7; (b2) calculated values from Ref. 7 including exchange correlation; (c) experimental values from Ref. 16, Table 7.4.

	α_Δ	α_Λ
(a) Calculation		
(15,59) LDA	0.49	0.37
(27,113) LDA	0.39	0.32
(15,59) EPM	0.59	0.69*
(b) Comparison with other work and experiment		
(a)	0.60	0.49
(b1)	0.49	0.49
(b2)	0.38	0.38
(c)	0.41	0.32

the experimentally observed anisotropy in the plasmon dispersion along the Δ and Λ axes. As remarked before, the EPM calculation does not reproduce this anisotropy. Besides, the EPM plasmon dispersion relation along the Λ axis cannot very well be described with Eq. (8). The first three rows of Table I(b) contain the values for α obtained in Refs. 15 and 7. The values of Ref. 15 have been obtained in a calculation in which the crystal potential was treated perturbatively. This calculation, which from a theoretical point of view is simpler than ours, also leads to an anisotropic dispersion. The values for α_Δ and α_Λ, however, are larger than the values obtained by us.

Because of the particular method of calculation, the plasmon energies in Ref. 7 had to be defined as the first moment (center of gravity) of the energy-loss function. This deviant definition of plasmon energies makes comparison with our results and experimental values problematic. For example, the use of the LDA in Ref. 7 yields an isotropic plasmon dispersion by definition, whereas our LDA calculation together with the common experimental definition of plasmon energies leads to an anisotropic dispersion.

Finally, the last row of Table I(b) contains the experimentally determined values for α_Δ and α_Λ as given in Ref. 16. The magnitude of the anisotropy in the values of α obtained in the (27,113) LDA calculation is in good agreement with the experimentally observed anisotropy.

In Figs. 2(a) and 2(b) we compare the calculated plasmon-resonance line shapes ($\mathrm{Im}[\epsilon^{-1}_{\mathbf{KK}}(\mathbf{k},\omega)]$ as a function of ω) for $\mathbf{k}\to\mathbf{0}$ with the experimental line shape of Ref. 17. We have checked the convergence of our results with respect to the size of the dielectric matrix as well as with respect to the number of plane waves. It turned out that as far as the loss function $\mathrm{Im}[\epsilon^{-1}_{\mathbf{KK}}(\mathbf{k}\to\mathbf{0},\omega)]$ is concerned a (15,169) calculation yields converged results.

Figure 2(a) is the result of a (59,169) EPM calculation. Figure 2(b) displays the results of two (15,169) LDA calculations, one of which without exchange-correlation corrections (full line) and the other with exchange-correlation corrections (dotted line). Comparing Fig. 2(a) with the full line in Fig. 2(b), we conclude that replacing the EPM band structure with a LDA band structure, without further inclusion of exchange-correlation effects, improves the width and the strength of the plasmon resonance as compared with experiment. The plasmon energy, however, is about 0.8 eV too large in both calculations. The dotted line in Fig. 2(b) shows that including exchange-correlation corrections in the LDA scheme does not give a further improvement; in fact, the agreement with experiment worsens.

We end this section with Fig. 3 in which we have plotted the complex plasmon energies $z(\mathbf{k})$ which are defined as the solutions of

$$\det[\epsilon(\mathbf{k},z)]=0\ . \tag{9}$$

In Ref. 1 we called this the theoretical definition. The full lines in the figure have been obtained by neglecting LFE, that is by disregarding the nondiagonal elements of ϵ in Eq. (9). This reduces Eq. (9) to the simpler equation

$$\epsilon_{\mathbf{KK}}(\mathbf{k},z)=0\ . \tag{10}$$

The solutions on the full line are labeled by the value of

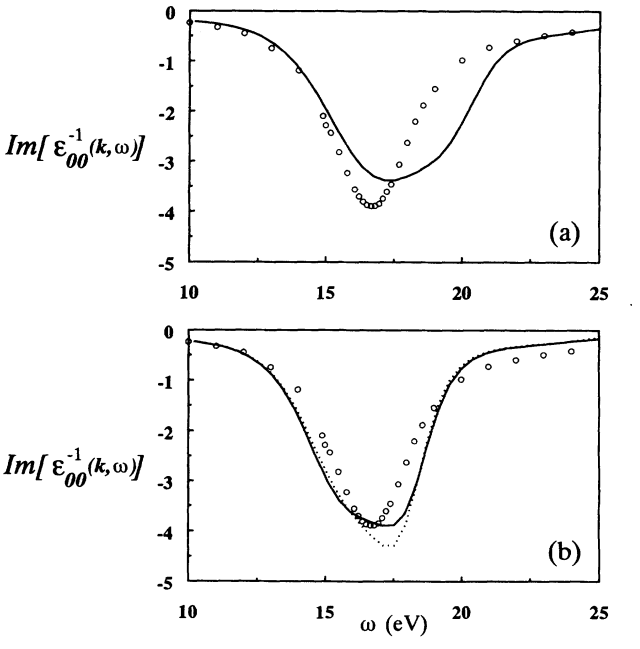

FIG. 2. Comparison of the results for $\mathrm{Im}[\epsilon^{-1}_{00}(\mathbf{k},\omega)]$ at $\mathbf{k}=(0,0.029,0.029)$ with experiment. The value of $\mathbf{k}$ is such that $|\mathbf{k}|=0.067$ Å^{-1} equals the value of the momentum transfer at which the experiments were performed. (a) (59,169) EPM calculation. (b) (15,169) LDA calculation. ——, no exchange-correlation corrections; · · · ·, RPA with exchange-correlation corrections according to Eq. (3); ○, experimental values according to Ref. 17.

$\mathbf{k}+\mathbf{K}=(t,t,t)$, which is the plasmon wave vector (momentum). The LFE couples two plasmons which have wave vectors differing a reciprocal-lattice vector and if a LFE is taken into account through solving Eq. (9) the "no-LFE" plasmon dispersion curve splits into two branches (plasmon bands) which are plotted as the dotted curves in Fig. 3. The labels on this two-branched dotted curve give the value of $\mathbf{k}=(t,t,t)$.

We observe that the effect of the LFE on the plasmon lifetime is qualitatively the same in the EPM and the LDA calculations: the lifetime of the "no-LFE plasmon" with a wave vector within the 1BZ decreases (the absolute value of the imaginary part of the solution increases) and the lifetime of the "no-LFE plasmon" with a wave vector outside the 1BZ increases. However, especially near the 1BZ edge, the effect is much larger in the EPM calculation. This is reflected in Fig. 4 in which the total energy-loss function at $\mathbf{k}=\mathbf{k}_L=(0.5,0.5,0.5)$ is analyzed in its two plasmon contributions according to (see Ref. 1)

$$\mathrm{Im}[\epsilon_{00}^{-1}(\mathbf{k},\omega)]\approx \mathrm{Im}\left[\frac{R_{00}^{1}(\mathbf{k})}{\omega-z_1(\mathbf{k})}+\frac{R_{00}^{2}(\mathbf{k})}{\omega-z_2(\mathbf{k})}\right]. \quad (11)$$

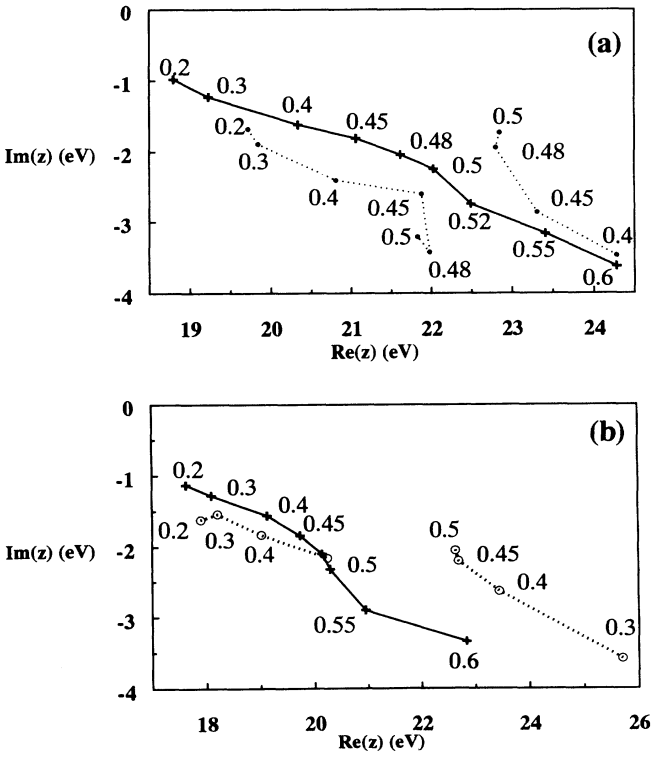

FIG. 3. Complex plasmon energies for $\mathbf{k}$ along the Λ axes. (a) has been obtained with an EPM calculation and (b) with a LDA calculation. The plasmon energies marked with + symbols have been obtained by neglecting local-field effects, that is, they are the solutions of $\epsilon_{\mathbf{KK}}(\mathbf{k},z)=0$. The numbers marking the + symbols give the value of $\mathbf{q}=\mathbf{k}+\mathbf{K}=(t,t,t)$. The ● symbols in (a) are the solutions of $\det[\epsilon(\mathbf{k},z)]=0$ using a (15,59) dielectric matrix. The ○ symbols in (b) were obtained using a (27,113) dielectric matrix. In these cases the labels give $\mathbf{k}=(t,t,t)$.

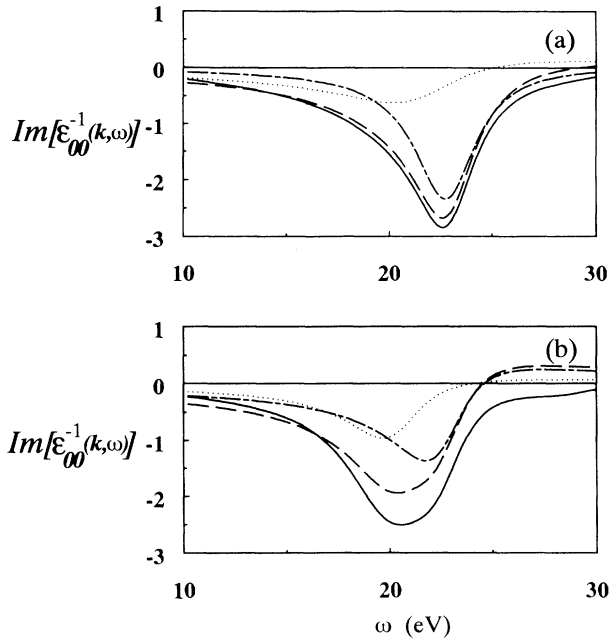

FIG. 4. This figure illustrates to what extent $\mathrm{Im}[\epsilon_{\mathbf{KK}}^{-1}(\mathbf{k},\omega)]$ and thus the energy-loss spectrum can be analyzed in plasmon resonances according to Eq. (11). The full lines in the figure correspond to $\mathrm{Im}[\epsilon_{00}^{-1}(\mathbf{k},\omega)]$. The dotted line and short-long-dashed line are the two terms of the right-hand side of Eq. (11); the long-dashed line is the sum of both. The figures correspond to the following calculations: (a) (15,59) EPM; $\mathbf{k}=(0.5,0.5,0.5)$. (b) (27,113) LDA; $\mathbf{k}=(0.5,0.5,0.5)$.

In this equation $z_1(\mathbf{k})$ and $z_2(\mathbf{k})$ are the solutions of Eq. (9), which were plotted in Fig. 3. $R_{00}^{1}(\mathbf{k})$ and $R_{00}^{2}(\mathbf{k})$ are the residues of the corresponding poles in ϵ^{-1}.

Figure 4(a) is identical to Fig. 9 of Ref. 1 and Fig. 4(b) is the analogous LDA figure. Due to the large difference in lifetime of the two EPM plasmons at $\mathbf{k}_L$—compare the two solutions at $\mathbf{k}=(0.5,0.5,0.5)$ in Fig. 3(a)—the first-band plasmon can hardly be recognized as a resonance in the energy-loss function of Fig. 4(a). In Fig. 4(b) we see that also in the LDA calculation, the contribution of the second-band plasmon is larger than the first-band plasmon contribution; the effect, however, is much less pronounced than in the EPM case.

IV. DISCUSSION AND CONCLUSIONS

We have presented the results of detailed LDA-based calculations of plasmon resonances in Si. Comparison with experiment clearly favors the use of a LDA band structure above an EPM band structure to calculate plasmon energies. In particular, in contrast to the EPM-based plasmon dispersion relations, the LDA-based plasmon dispersion relations along the Δ and Λ axes of the 1BZ show the correct anisotropic behavior. The LDA calculation, as well as the EPM calculation, gives rise to a plasmon dispersion which is too strong at large wave vectors.

In both calculations, EPM as well as LDA, there

remains a discrepancy of about 0.8 eV between the measured and the calculated plasmon energy at $\mathbf{k}=\mathbf{0}$. This difference cannot be explained by our neglect of the contribution of the core electrons to the polarizability. Although the correction on the plasmon energy due to these core electrons has the proper sign, its estimated value of -0.5% of the plasmon energy (-0.09 eV) as given in Ref. 7 is too small to account for the observed discrepancy. It is puzzling that the value of 16.6 eV, which is obtained by using the simple formula $E_{\rm pl}=\hbar(\rho e^2/m\epsilon_0)^{1/2}$ for the plasmon energy of a homogeneous system with ρ the mean electron density in Si, is much closer to the experimental 16.7 eV than our laboriously obtained value of 17.5 eV.

Concerning the shape of the loss function $\mathrm{Im}[\epsilon_{00}^{-1}(\mathbf{k}\rightarrow\mathbf{0},\omega)]$ we have seen that the LDA calculation leads to better agreement with experiment than the EPM calculations. In this case inclusion of exchange-correlation effects only changes the strength of the resonance and in fact worsens the agreement with experiment.

From our results it is clear that it is the mere replacement in Eq. (4) of the EPM band structure by the LDA band structure which yields the improved agreement with experiment. The further inclusion, as in Eq. (3), of the LDA-type exchange-correlation corrections in the dielectric matrix either worsens the agreement with experiment, as is the case with the loss function for $\mathbf{k}\rightarrow\mathbf{0}$, or hardly has any effect, as on the plasmon dispersion relation. This lack of effect on the plasmon dispersion relation, especially at large wave vectors, is probably due to the aforementioned two shortcomings in our scheme for including exchange-correlation corrections, which are the ω and $\mathbf{k}$ independence of the term $(\delta V_{\rm xc}/\delta\rho)$.

The objection of the ω independence of $(\delta V_{\rm xc}/\delta\rho)$ can possibly be met by using the energy-dependent DFT as described in Ref. 18. A way to use this theory in a LDA framework is suggested in Ref. 19. In principle the $\mathbf{k}$ dependence can be accounted for by doing a DFT calculation without making the LDA. Of course this requires a suitable nonlocal exchange-correlation functional which can for example be found in Ref. 20.

As shown in Eq. (11) and Fig. 4 our method of calculation enables us to identify explicitly the plasmon poles in the inverse dielectric matrix and to obtain the plasmon contribution to the inverse dielectric matrix. This reminds one of the plasmon-pole models occurring in the *GW* approximation, which has successfully been used in semiconductor band-structure calculations (e.g., Refs. 21–23). However, contrary to the real-valued plasmon-pole positions in those models, the pole positions as we calculate them have a finite imaginary part corresponding to the inverse resonance lifetime. Therefore, in the region of the plasmon energy, our representation in Eq. (11) is a far better approximation to the inverse dielectric matrix than the above-mentioned models. On the other hand, the plasmon-pole models are not devised to describe the plasmon resonance in detail, but are meant to give a convenient and accurate description of the inverse dielectric matrix at low frequencies. In fact, the static dielectric matrix is used as input to obtain the pole parameters. It is clear that the representation in Eq. (11) does not make sense at frequencies too far from the plasmon frequency, in particular not at low frequencies. Therefore, considered from a *GW* point of view, our pole parameters are not to be considered an improvement over the parameters of the plasmon-pole models. However, in Ref. 24 it is suggested how to extend the representation in Eq. (11) in order to give it a larger range of validity. Results illustrating this extended representation in a one-dimensional model system can be found in Ref. 25.

To conclude, we think that we have come far in performing an *ab initio* calculation of dielectric matrices and related quantities of an inhomogeneous system like silicon. The remaining discrepancies between our results and experiments cannot be resolved by increasing the number of plane waves or the size of the dielectric matrix, but requires the use of more elaborate schemes to account for exchange-correlation corrections.

ACKNOWLEDGMENTS

B.F. is supported in part by Girton College, Cambridge, and the Science and Engineering Research Council of the United Kingdom.

*Present address: Koninklijke/Shell-laboratorium, Amsterdam, Badhuisweg 3, 1031 CM Amsterdam, The Netherlands.

[1]R. Daling, W. van Haeringen, and B. Farid, Phys. Rev. B **44**, 2952 (1991).
[2]P. Nozières and D. Pines, Phys. Rev. **113**, 1254 (1959).
[3]P. Vashista and K. S. Singwi, Phys. Rev. B **6**, 875 (1972).
[4]J. T. Devreese, F. Brosens, and L. F. Lemmens, Phys. Rev. B **21**, 1349 (1980); **21**, 1363 (1980).
[5]P. K. Aravind, A. Holas, and K. S. Singwi, Phys. Rev. B **25**, 561 (1982).
[6]K. Utsumi and S. Ichimaru, Phys. Rev. B **23**, 3291 (1981).
[7]M. Taut, J. Phys. C **19**, 6009 (1986).
[8]S. P. Singhal and J. Callaway, Phys. Rev. B **14**, 2347 (1976).
[9]P. J. H. Denteneer, Ph.D thesis, Eindhoven University of Technology, The Netherlands, 1987. P. J. H. Denteneer and W. van Haeringen, J. Phys. C **18**, 4127 (1985).
[10]W. Kohn and L. J. Sham, Phys. Rev. **140**, A1133 (1965).
[11]E. P. Wigner, Phys. Rev. **46**, 1002 (1934).
[12]G. B. Bachelet, H. S. Greenside, G. A. Baraff, and M. Schlüter, Phys. Rev. B **24**, 4745 (1981).
[13]J. Stiebling and H. Raether, Phys. Rev. Lett. **40**, 1293 (1978).
[14]C. H. Chen, A. E. Meixner, and B. M. Kincaid, Phys. Rev. Lett. **44**, 951 (1980).
[15]K. Sturm, Adv. Phys. **31**, 1 (1982).
[16]H. Raether, *Excitations of Plasmons and Interband Transitions by Electrons,* edited by G. Höhler, Springer Tracts in Modern Physics Vol. 88 (Springer-Verlag, Berlin, 1980).
[17]J. Stiebling, Z. Phys. B **31**, 355 (1978).
[18]E. Runge and E. K. U. Gross, Phys. Rev. Lett. **52**, 997 (1984).
[19]E. K. U. Gross and W. Kohn, Phys. Rev. Lett. **55**, 2850 (1985).
[20]D. C. Langreth and M. J. Mehl, Phys. Rev. B **28**, 1809 (1983).

[21]M. S. Hybertsen and S. G. Louie, Phys. Rev. B **34**, 5390 (1986).
[22]W. von der Linden and P. Horsch, Phys. Rev. B **37**, 10 159 (1988).
[23]N. Hamada, N. Hwang, and A. J. Freeman, Phys. Rev. B **41**, 3620 (1990).
[24]B. Farid, G. E. Engel, R. Daling, and W. van Haeringen, Phys. Rev. B **44**, 13 349 (1991).
[25]G. E. Engel, B. Farid, C. M. N. Nex, and N. H. March, Phys. Rev. B **44**, 13 356 (1991).